22. REMAGNETIZED SEDIMENTS AT DEEP SEA DRILLING PROJECT SITES 467 AND 471[1]

C. R. Denham, H. G. Farmer, and A. Shaughnessy, Department of Geology and Geophysics,
Woods Hole Oceanographic Institution, Woods Hole, Massachusetts

INTRODUCTION

We conducted paleomagnetic measurements on the thick, Neogene sedimentary sections at DSDP-IPOD Leg 63 Site 467 (San Miguel Gap) and Site 471 (west of the foot of Baja California) (see Sites 467 and 471 chapters, this volume) in order to date and correlate them on the basis of their magnetic polarity stratigraphy. These two sections are much thicker and much more thoroughly sampled than the sediments at the other Leg 63 sites. This report describes the measurements, presented largely in tabular form, from which we have inferred that Sites 467 and 471 do not bear useful polarity stratigraphies. These sediments have been remagnetized, with virtually all their present magnetization being normally polarized (i.e., inclined downwards). Remagnetization is clearly demonstrated in a highly folded interval near the bottom of Hole 467. Although the two sites are more than 10° apart in latitude, they show the same value and dispersion of remanent magnetic inclination; the geocentric axial dipole and present-day values for the region are statistically included within the data. An analysis of magnetic directions for pairs of specimens from unbroken pieces of core shows that the present weak, but moderately stable, remanence can be measured reliably with a sensitive cryogenic magnetometer and a clean, alternating-field demagnetizer.

METHODS

The paleomagnetic specimens were small cylinders 2.54 cm in diameter and length. They were extracted from the center of the split face of the working half of the core, using a water-cooled, diamond-tipped core drill and trimmed with a diamond saw. The samples were kept wet until they were measured. The sediments were too weakly magnetized to be measured with the onboard Digico spinner magnetometer. We measured their remanence with our Superconducting Technology C-102 two-axis cryogenic rock magnetometer, whose effective noise level is about 3×10^{-8} Gauss-cm^3. The magnetic cleaning was done with a Schonstedt GSD-1 alternating-field (AF) demagnetizer. Both of these apparatuses have had a long history of very high-quality behavior in our laboratory.

The samples were collected from subhorizontally bedded, lithified units. The apparent dip on the split-face of the core was measured at or near each specimen, in case a dip correction should become necessary to interpret the polarities. A few samples were taken in more steeply dipping strata for paleomagnetic fold testing, notably in Core 99 of Hole 467.

To remain continually aware of the appropriate AF demagnetization field, we conducted frequent progressive demagnetizations, and almost all of the samples were treated at least in 100 and 200 oe-peak AF, rather than in only a single-peak field. Tables 1 and 2 show the remanent magnetizations before any AF treatment was done, and again after the 200-oe treatment was applied. Generally, the intensities of natural magnetic remanence were sharply reduced by the 200-oe cleaning. The magnetic directions were moderately stable, changing ~10° to 20° as a result of the 200-oe treatment. The magnetic directions for pairs of adjacent samples from unbroken core pieces were internally similar, as the following material describes.

SITE 467 (SAN MIGUEL GAP: 33°51′W, 120°45′W)

A total of 176 indurated specimens was measured (Table 1) at Site 467, almost all of these from middle to upper Miocene Cores 57 to 101, spanning 528.5 to 956 meters depth below the seafloor. Forty cores are represented (Table 1). Only 15 of the specimens have upwardly inclined (reversed) magnetic inclinations. Two reversed features are worth noting.

All four specimens from the clayey limestone unit penetrated by Core 60, Sections 1 to 2, are reversely magnetized, averaging −31° inclination. The reversed polarity was present over the 50- to 300-oe peak AF range, beyond which the remanence was too weak to measure. In Core 79, Section 3, a pair of samples from an unbroken core piece show a polarity reversal with a directional change of 166°.

Evidently, minor portions of the Site 467 sedimentary column are capable of preserving ancient reversal information. Generally speaking, however, none of the original paleomagnetic remanence exists any longer. Were the opposite to be true, then the sediments would have been roughly equally divided between normal and reversed polarity, and some twenty polarity reversals would have been seen in the 6 to 14 m.y. spanned by Cores 57 to 101 (e.g., Ness et al., 1980). The likelihood that we would have sampled so few reversed horizons by mere coincidence is nil.

The average absolute value of magnetic inclination, giving equal weight to each of the 41 cores, is 52°, with a standard deviation of ±11°. The standard error on the mean is 2°. By comparison, the expected geocentric axial dipole field inclination is 53°, and the present-day inclination is 59°; both are within the 67% confidence interval of the data. Indeed, the data and the axial dipole value are statistically indistinguishable.

Pair-wise Dissimilarity

Twenty-five pairs of samples from unbroken pieces of core were measured to check the reliability of the sampling and laboratory methods. Using the measure $\delta = \cos^{-1}(R/N)$, where N is the number of samples in the cluster (= 2) and R is the sum of the unit-vector magnetic directions in each cluster, the average dissimilarity

[1] *Initial Reports of the Deep Sea Drilling Project*, Volume 63.

Table 1. Site 467 remanent magnetism before AF cleaning and after cleaning at 200-oe peak AF.

Core	Section	Depth in Hole to Top of Section (m)	Interval Sampled within Section (m)	Samples from Continuous Segment of Core	NRM			200 oe					
					Incl	Decl	Int	Incl	Decl	Int	$\delta = \cos^{-1}(R/N)$	Remarks	200 oe $\|\bar{I}\|$
33	3	303.5	84–86		−17	169	2.4	58	114	0.5			58
36	4	333.5	68–70		20	338	3.4	23	328	1.2			23
40	1	267.0	67–69		42	108	4.4	59	122	2.3			59
57	1	528.5	70–72		41	314	4.0	72	21	1.0			53 ± 11
	1		129–131		39	357	4.3	55	338	1.1			
	2	530.0	98–100		18	31	4.2	38	43	1.2			
	2		116–118		30	6	3.7	53	0	0.9			
	3	531.5	4–6		55	180	4.5	54	185	0.9			
	3		146–148		23	358	4.9	41	16	1.1			
	4	533.0	118–120		40	355	2.9	61	256	0.7			
	4		138–140		35	320	3.2	52	275	1.1			
58	1	538.0	11–13		80	41	2.4	67	180	0.8	12°		49 ± 13
	1		81–84		69	72	1.7	44	176	0.8			
	1		108–111		41	1	4.3	42	0	1.2			
	2	539.5	26–28		67	69	3.1	72	127	1.0			
	2		61–63		16	28	5.5	39	34	1.0			
	2		101–103		30	113	4.5	45	143	0.6			
	2		131–133		36	20	6.8	43	16	1.6			
	4	542.5	22–24		13	31	3.8	38	13	0.8			
59	1	547.5	32–34		53	344	4.1	53	17	1.6			
	1		77–79		26	7	6.0	50	0	1.9			
	2	549.0	36–38		7	19	3.4	66	57	0.9			56 ± 8
60	1	557.0	130–132		9	86	1.7	−30	73	1.7		Reversed for 50–300 oe	31 ± 14
	2	558.5	18–20		−25	77	16.8	−44	86	11.6		clayey limestone	
	2		41–43		−1	19	2.8	−42	26	0.9			
	2		52–54		47	82	1.6	−10	38	0.4			
61	1	566.5	28–30		3	37	1.0	38	25	0.7			53 ± 21
	1		87–89		50	326	5.6	68	318	1.1			
62	1	576.0	19–21		51	337	4.7	78	335	1.4			57 ± 18
	1		36–38		38	20	8.0	49	51	1.2			
	1		90–92		11	31	6.6	45	67	1.4			
63	1	585.5	18–20		20	65	1.3	79	220	0.3	16°		57 ± 12
	1		38–40		−29	81	1.3	54	175	0.4			
	1		59–61		38	108	1.8	41	164	0.8	$k = 19$		
	1		77–79		73	53	1.3	52	181	0.5			
	1		108–110		44	8	2.4	54	189	0.5			
	2	587.0	9–11		36	0	4.2	54	355	1.4	11°		
	2		86–88		71	57	1.7	62	34	0.6			
65	1	604.5	96–98		51	75	4.7	62	82	0.7	7°		66 ± 6
	1		104–106		12	31	3.9	72	104	0.6			
	2	606.0	26–28		30	55	6.2	63	71	0.8			
66	1	614.0	27–29		−39	325	6.5	−69	314	1.5			78 ± 13
	1		73–75		75	273	5.0	87	246	2.5		100 oe demag	
67	1	623.5	38–40		9	271	1.1	−82	124	0.9		$I = -83°$ $D = 261°$@ 100 oe demag	41 ± 58
	1		136–138		−32	51	1.6	0	50	0.7		100 oe demag	
68	1	633.0	141–143		55	355	11.1						39 ± 30
	2	634.5	1–3		54	292	13.6	60	303	0.9			
	2		40–42		19	328	11.9	17	301	2.5			
69	1	642.5	44–46		21	3	2.7	26	5	0.5			32 ± 10
	2	644.0	69–71		80	250	0.9	44	249	0.6			
	3	645.5	35–37		−14	154	1.4	26	160	0.2			
70	1	652.0	27–29		−67	355	4.5	−69	5	0.5			46 ± 20
	2	653.5	72–74		32	225	0.5	34	251	0.2			
	3	645.0	13–15		−10	41	1.2	−35	165	0.4			
74	1	690.0	4–6		65	200	1.6	50	202	0.3			39 ± 16
	2	691.5	1–3		26	344	4.3	28	316	0.7			
75	1	699.5	8–10		8	339	0.4	44	332	0.3		100 oe demag	44
76	1	709.0	27–29		23	35	0.9	39	4	0.2			49 ± 8
	1		147–149		47	74	0.6	54	100	0.2			
	2	710.5	34–36		49	68	0.9	53	131	0.3			
77	1	718.5	66–68		−3	50	1.7	−3	22	0.3			54 ± 29
	1		89–91		65	19	2.1	69	10	1.3		100 oe demag	
	1		130–132		47	17	2.5	68	82	0.7			
	2	720.0	19–21		41	39	1.6	62	63	0.7		100 oe demag	
	2		81–83		65	140	3.1	69	172	1.1			
78	1	728.0	26–28		5	71	3.5	−3	49	0.6			39 ± 49
	1		73–75		58	30	0.7	72	119	0.1			
79	1	737.5	68–70		58	300	2.1	57	284	0.6			61 ± 7
	1		83–85		40	352	7.9	55	349	3.5			
	2	739.0	21–23		50	128	12.9	52	118	5.3			
	2		76–78		42	61	6.6	59	103	2.6			
	2		88–90		48	53	14.0	57	66	4.4	10°		
	2		138–140		58	37	22.7	63	58	6.1			
	3	740.5	70–72		−61	72	25.1	−57	71	10.7		Reversal boundary?	
	3		132–134		63	332	1.3	69	265	0.5			
	4	742.0	16–18		56	9	13.9	62	9	5.9			
	4		105–107		58	57	7.3	70	58	4.6			
	5	743.5	25–27		84	174	15.6	73	204	10.3			
80	1	747.0	15–17		25	161	7.9	52	128	1.3	13°		60 ± 11
	1		30–32		50	159	15.5	68	83	2.5			
83	1	775.5	7–9		52	219	6.0	57	267	1.7			52 ± 10
	1		105–107		51	169	4.3	54	184	1.3			
	2	777.0	79–81		37	345	2.3	48	300	0.8			
	2		139–141		16	195	4.5	45	223	1.4			
	3	778.5	44–46		26	6	4.4	39	21	0.9			
	3		92–94		60	265	3.6	65	287	1.5			
	4	780.0	37–39		58	147	2.3	63	148	0.8			
	4		86–88		36	15	1.3	43	16	0.8			
84	1	785.0	8–10		24	53	1.5	65	53	0.7			58 ± 13
	1		12–14		69	145	2.2	−28	201	1.6			
	1		47–49		43	34	6.3	57	86	1.4	11°		

Table 1. (Continued).

Core	Section	Depth in Hole to Top of Section (m)	Interval Sampled within Section (m)	Samples from Continuous Segment of Core	NRM Incl	NRM Decl	NRM Int	200 oe Incl	200 oe Decl	200 oe Int	$\delta = \cos^{-1}(R/N)$	Remarks	200 oe $\lvert\bar{I}\rvert$
	1		74-76		46	104	1.9	72	43	0.5	11°		
	2	786.5	24-26		38	38	1.4	52	15	0.5			
	2		58-60		38	25	4.2	47	25	1.6			
	2		75-77		81	22	2.2	63	0	1.1	7°		
	2		91-93		42	23	3.9	53	15	1.3	$k = 107$		
	2		101-103		55	28	3.0	54	16	1.0			
	3	788.0	36-38		65	174	2.4	72	13	0.9			
	2		133-135		41	113	2.9	49	110	0.9			
	4	789.5	46-48		78	21	2.0	74	55	0.8			
	4		97-99		67	126	3.3	68	96	0.9			
85	1	794.5	17-19		28	17	8.9	42	29	2.4	13°		60 ± 12
	1		41-43		50	7	5.8	66	10	1.5			
	1		105-107		63	30	6.3	58	30	1.9	9°		
	1		121-123		51	123	3.7	41	17	2.2			
	2	796.0	24-26		62	170	8.2	77	15	1.8	13°		
	2		53-55		45	10	1.3	53	348	0.8			
	3	797.5	47-49		80	286	2.4	57	330	1.1	3°		
	3		81-83		37	321	4.9	53	339	2.1			
	3		118-120		82	99	9.2	71	10	3.4	19°		
	3		133-135		62	117	5.2	69	161	0.6			
	4	799.0	50-52		53	109	6.7	72	41	2.0	20°		
	4		72-74		38	177	4.4	66	185	1.2			
	5	800.5	76-78		59	123	7.9	71	256	2.3	8°		65 ± 9
	5		95-97		19	333	2.8	58	276	1.7			
86	1	804.0	92-94		47	340	2.7	58	294	1.2	16°		59 ± 21
	1		108-110		48	59	7.5	88	45	2.4			
	2	805.5	4-6		34	356	13.9	66	19	3.3			
	3	807.0	22-24		−42	240	8.2	−17	195	1.3	35°		
	3		58-60		43	158	1.5	53	154	1.1			
	4	808.5	76-78		62	234	2.6	67	245	1.1	4°		
	4		107-109		65	293	2.3	62	257	1.3			
87	1	813.5	73-75		56	34	5.7	47	26	1.7	5°		61 ± 7
	1		90-92		41	16	5.9	55	19	2.0			
	2	815.0	52-54		47	2	6.1	58	36	1.9			
	2		142-144		63	147	6.0	61	158	1.5			
	3	8.6.5	58-60		62	102	5.7	69	132	2.0	2°		
	3		93-95		56	87	7.4	68	122	3.0			
	4	818.0	30-32		53	343	6.6	57	308	1.8	4°		
	4		95-98		37	344	8.4	59	321	2.0			
	5	819.5	73-75		51	334	3.3	68	317	1.3	7°		
	5		99-101		67	152	2.1	70	279	1.4			
91	1	851.5	20-22		49	88	2.4	61	175	1.1			63 ± 12
	1		70-72		72	90	24.2	46	72	6.2			
	3	854.5	18-20		65	223	8.3	50	214	3.0			
	3		31-33		76	33	3.9	76	156	1.3			
	5	857.5	25-27		59	222	4.4	69	235	1.6			
	5		38-40		49	299	2.4	73	268	0.9			
92	1	861.0	42-44		34	345	1.4	45	356	0.9			45
93	1	870.5	103-105		41	332	5.5	58	356	1.5			53 ± 14
	1		105-108		37	351	4.6	51	333	1.6			
	3	873.5	37-39		49	99	5.5	31	113	3.2			
	3		71-73		78	306	3.6	69	225	1.7			
	4	875.0	8-11		36	87	2.8	45	112	0.8	15°		
	4		28-31		40	65	4.0	62	70	1.2			
94	1	880.0	82-84		57	183	2.9	55	153	1.5			44 ± 28
	1		91-93		2	313	20.0	38	307	2.7			
	2	881.5	58-60		50	300	4.6	62	266	1.6			
	2		76-78		65	41	2.8	67	67	1.5			
95	1	889.5	18-20		25	94	8.9	43	108	2.4			43 ± 25
	1		27-29		60	145	5.7	54	133	1.7			
96	1	899.0	7-9		−44	355	5.7	−43	4	2.0			43 ± 6
	1		15-17		−49	224	5.3	−50	249	1.1			
	2	900.5	63-65		37	145	12.1	43	132	3.4			
97	3	911.5	75-77		66	84	6.0	54	93	2.4			61 ± 5
	3		86-88		57	121	8.9	56	83	3.0			
	3		102-104		60	50	11.4	59	57	4.1			
98	1	918.0	36-38		63	310	6.1	69	295	2.4	13°		
	1		50-52		31	293	7.1	46	274	2.9			
99	1	927.5	59-61		65	179	9.1	66	186	2.8			64 ± 22
	1		73-75	A	71	357	3.9A	52	185	1.5		Fold	
	1		89-91	B	77	290	7.2B	75	248	2.3	13°	$N = 6$	
	1		93-95	C	17	266	5.5C	66	232	2.5		$S = 13°$	
	1		104-106	D	63	142	6.8D	51	182	2.5	$k = 33$	$k = 31$	
	1		109-111	E	77	351	4.3E	70	202	2.1		$\bar{I} = 64.4°$	
	1		119-121	F	81	249	5.4F	62	193	2.4		$\bar{D} = 200.2°$	
	2	929.0	77-79		39	49	8.4	46	22	2.4			56 ± 9
	2		93-95		55	14	10.2	66	8	3.7	9°		
	2		113-115		55	22	9.3	58	21	3.1	$k = 61$		
	2		131-133		49	21	9.0	48	22	3.4			
	3	930.5	71-73		58	205	7.2	61	196	2.6			
100	1	937.0	7-9		68	338	6.8	77	277	2.4	5°		63 ± 18
	1		12-14		68	320	7.3	69	257	2.7			
	2	938.5	7-9		25	29	8.4	43	41	3.3			
101	1	946.5	5-7		68	166	4.2	59	204	2.2	7°		60 ± 1
	1		19-21		55	92	3.9	60	178	2.1			
Mean Value													$\lvert I\rvert = 52 \pm 11$

Note: Lat: 33°51′, Long: 120°45′. GAD I = 53.3°. Present I = 59°. Inclination is positive downward; declination advances eastward from north, relative to the split face of the working core half. Incl. = 0°, Decl. = 0° is horizontal and directed into the split face. The angular dispersion δ is $\cos^{-1}(R/N)$, where R is the unit-vector sum of directions for the cluster, and N is the number of samples in the cluster. The average of absolute inclinations $\lvert\bar{I}\rvert$ is also given. All angles are in degrees; intensities are in units of 10^{-7} Gauss.

was $\delta = 11°$, with a standard deviation of $\pm 7°$. This δ value remained the same when three larger clusters ($N > 2$) were also included.

The pair-wise dispersions are small. If we were to assume that all the pairs were drawn from the same Fisherian population with constant precision parameter k, then these data would suggest crudely a k value of about 19. The median δ value is 11°, equivalent to $R = 1.963$. This is the median R value for pairs drawn from a $k = 19$ population, as estimated using Fisher's (1953, p. 302) formula for the unconditional distribution of R when $N = 2$:

$$\text{Prob}\ (R < R_o;\ N = 2) = \frac{\cosh\ (kR_o) - 1}{\sinh^2 k}$$

This $k = 19$ is a very crude estimate of the noisiness of these data. It corresponds to a 16° median deviation from the mean direction at any horizon. That is, if the errors are Fisherian distributed with $k = 19$, then half the measurements will lie within 16° of the actual mean direction, and 95% of them will lie within 33° of the mean. We conclude from this pair test that the present-day magnetization is roughly constant over short vertical distances at Site 467, and that we have measured it accurately.

The sources of dissimilarity are orientation errors, measurement errors, geomagnetic secular variation, and spurious viscous magnetization acquired during drilling, preparation, and storage of the specimens. Overall, the results here are as precise and accurate as can be reasonably expected for rotary drilled, azimuthally unoriented, weakly magnetized specimens.

Fold Test

In Core 99, Section 1, a long, unbroken piece of core penetrated several limbs of a complex slump feature, which was sampled for a fold test (Graham, 1949) (Fig. 1 and Table 1). Specimen 73–75 cm appears to be overturned with respect to 93–95 cm; 104–106 cm is overturned with respect to 119–121 cm. Yet the former pair differ in magnetic direction by only 27°, the latter by only 13°. Specimens at 89–91 cm and 109–111 cm are from the apparent fold axes. They each have a complicated internal structure, yet even they differ magnetically only by 14°. The magnetic directions lie in an area 9° wide by 35° long.

Taken all together, the six specimens in the slump have a precision parameter of $k = 31$, indicative of moderately tight clustering despite the highly contorted layering. The inclination of the mean direction is 64°, with $\alpha_{95} = 12°$. This mean inclination and cone of confidence include the mean inclination for all the data, as well as the axial dipole and present-day inclinations. When the beds are corrected to a horizontal attitude by the most direct path, ignoring the overturning, k falls to 6. At 95% confidence, this is statistically different from $k = 31$ (McFadden, 1980; Cox, 1969). With overturning, k is less than 2 and not significant at the 5% level (Watson, 1956).

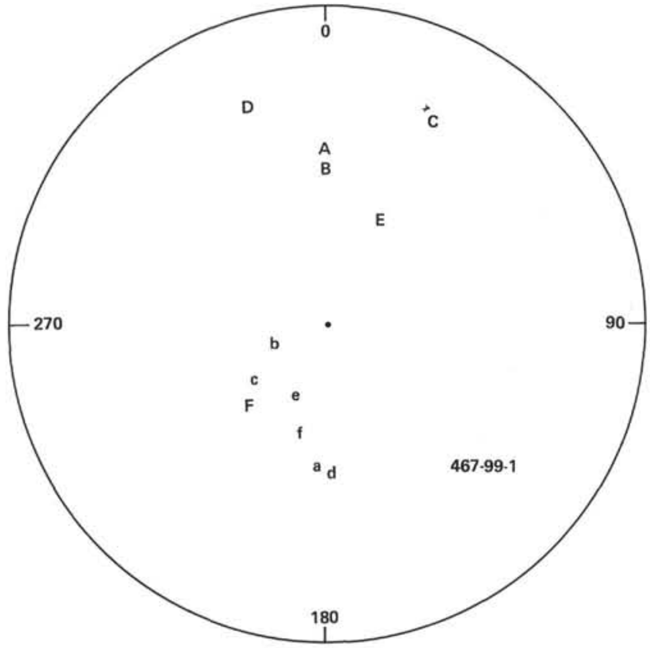

Figure 1. Bedding orientation poles (A–F) and corresponding structurally uncorrected remanent magnetic directions (a–f), cleaned at 200-oe peak AF, for a slump feature at DSDP Site 467, Core 99, Section 1. (Equal-area projection, with declination relative to the split face of the working core half; 0° is directed into the split face. The magnetic directions [a–f] lie on the lower hemisphere in a narrow area in the southwest quadrant [see Table 1]. The bedding poles [A–F] are upwardly normal to the present folded beds. Beds C and F actually are overturned; their original upward poles can be obtained by reflection through the center of the unit sphere. For the magnetic directions shown here, $N = 6$, $R = 5.84$, and $k = (N - 1)/(N - R) = 31$. Structural reorientation to a horizontal attitude causes R to fall to 5.2 or less, k to 6 or less, depending on the reorientation scheme used [see text]. The latter imply significantly greater dispersion at the 95% confidence level [McFadden, 1980; Cox, 1969]. Evidently, the observed magnetic directions were acquired after the folding occurred.)

The sediment magnetization appears to have been acquired after the slumping occurred. If this were not so, then some of the remanent magnetic directions would have been inverted onto the upper hemisphere by the folding process. The k value would have been larger after correction to a horizontal attitude, rather than before. Instead, the opposite is observed, implying post-folding magnetization. This test proves only that this particular portion of the site was remagnetized. It suggests that this remagnetization occurred for other levels as well. It does not, however, distinguish between a chemical and a post-detrital model of remagnetization (e.g., Niitsuma, 1977).

SITE 471 (WEST OF THE FOOT OF BAJA CALIFORNIA: 23°29′N, 112°30′W)

The paleomagnetic story for Site 471 is the same as for Site 467 (Table 2). Of 135 indurated specimens from 31 middle Miocene cores (34–78; 313.5–741 m sub-bottom depth), only eight are reversely magnetized, and four of those trended strongly toward normal polarity during AF cleaning.

Table 2. Site 471 remanent magnetism before AF cleaning and after cleaning at 200-oe peak AF.

Core	Section	Depth in Hole to Top of Section (m)	Interval Sampled within Section (cm)	Samples from Continuous Segment of Core	NRM Incl	NRM Decl	NRM Int	200 oe Incl	200 oe Decl	200 oe Int	$\delta = \cos^{-1}$ (R/N)	Remarks	200 oe $\lvert\bar{I}\rvert$
34	1	313.5	13–15		15	87	3.7	71	32	1.8			55 ± 17
	1		49–51		−84	355	18.9	−73	32	2.4		Reversal?	
	1		65–67		70	104	5.7	48	158	1.6			
	1		80–82		49	214	4.7	59	20	2.2			
	2	315.0	26–28		45	156	13.2	46	113	2.9			
	3	316.5	6–8		6	348	26.6	25	353	4.3	32°		
	3		15–17		77	3	12.8	62	336	4.3			
35	1	323.0	17–19		23	158	22.5	24	157	8.0			53 ± 22
	1		138–140		35	176	18.8	54	334	4.6			
	2	324.5	44–46		59	181	36.9	77	229	6.3			
	2		48–50		44	223	19.6	57	312	5.8			
36	1	332.5	115–117		−13	233	25.0	6	198	5.0			30 ± 18
	1		123–125		20	0	21.9	45	310	4.8			
	2	334.0	16–18		19	174	19.5	27	176	5.4	7°		
	2		22–24		73	216	12.3	41	177	5.4			
37	1	342.0	48–50		56	290	11.6	47	228	4.4			41 ± 7
	1		56–58		46	200	13.8	30	194	6.1			
	1		126–128		39	2	22.3	41	356	6.7	5°		
	1		131–133		30	348	20.2	40	342	6.3			
	2	343.5	16–18		55	93	14.5	52	71	5.7	6°		
	2		26–28		36	44	19.7	40	72	6.1			
	2		95–97		33	359	15.4	35	353	4.6	3°		
	2		103–105		35	2	14.0	40	354	4.5			
38	1	351.5	21–23		65	59	10.6	55	132	3.4	9°		50 ± 17
	1		27–29		38	88	11.3	42	113	3.6			
	1		88–90		30	124	8.9	46	104	3.4			
	2	353.0	74–76		60	36	8.3	75	84	2.8			
	2		80–82		22	337	6.7	30	318	2.3			
39	1	361.0	90–92		45	144	13.5	52	113	4.5	13°		50 ± 3
	1		96–98		50	50	14.5	48	74	5.0			
42	1	389.5	48–50		41	12	25.9	62	166	5.0			62
43	1	399.0	1–3		55	80	19.0	54	117	8.0			62 ± 10
	1		6–8		28	96	17.3	35	112	5.8			
	4	403.5	134–136		71	322	12.4	75	250	4.0			
44	3	411.5	26–28		83	161	4.9	65	155	1.6			65
46	2	429.0	41–43		53	19	18.9	64	39	5.1			60 ± 10
	2		64–66		−68	33	5.4	−70	110	1.1	10°		
	2		68–70		−43	101	5.5	−51	108	1.3			
47	1	437.0	49–51		66	350	10.1	84	21	3.6			76 ± 12
	2	438.5	13–15		53	45	12.9	67	69	4.0			
48	1	446.5	89–91		42	87	9.9	46	79	2.7			
	1		94–96		44	93	4.8	47	54	0.9			47 ± 1
	3	449.5	41–43		34	51	11.4	48	67	3.5			
50	1	465.5	49–51		61	48	15.7	57	66	3.8	28°		49 ± 9
	1		55–57		65	323	20.7	60	192	3.0			
	2	467.0	87–89		25	358	10.7	40	354	4.7		100 oe demag	
	4	470.0	46–48		44	272	11.3	45	248	3.9	8°		
	4		52–54		48	245	11.2	45	225	5.3			
51	1	475.0	30–32		12	27	24.4	29	38	5.2			44 ± 14
	1		35–37		53	318	34.6	51	334	9.2			
	2	476.5	51–53		18	163	16.2	44	170	5.0	9°		
	2		60–62		14	162	19.0	26	170	4.6			
	2		115–117		44	164	20.6	56	154	4.2			
	3	478.0	127–129		35	197	18.1	58	230	2.8			
52	1	484.5	109–111		86	235	19.0	79	317	6.1			75 ± 9
	1		124–126		43	212	12.3	70	225	4.5			
	2	486.0	49–51		88		9.5	82	193	3.9			
	3	487.5	22–24		43	216	13.4	59	225	4.2			
	3		82–84		77	60	10.8	82	82	3.9	6°		
	3		86–88		73	3	13.8	77	14	4.7			
53	2	495.5	91–93		38	55	26.3	48	54	7.7			55 ± 9
	2		107–109		17	223	34.6	61	257	3.6			
	3	497.0	54–56		59	256	15.6	73	297	4.7			74 ± 6
	4	498.5	10–12		59	223	13.7	81	221	4.6	6°		
	4		25–27		20	265	21.1	69	207	4.3			
57	1	532.0	19–21		32	216	17.1	40	246	5.7	8°		48 ± 11
	1		23–25		49	202	25.0	56	245	6.0			
58	1	541.5	95–97		33	342	21.9	73	328	4.6			51 ± 31
	3	544.5	98–100					29	350	5.7			
59	1	551.0	57–59		−76	35	28.5	−14	41	3.0		Continued to normal at high demag (42°*I* at 300 oe)	37 ± 18
	1		139–141		50	85	16.0	56	96	4.4			
	2	552.5	62–64		39	315	22.4	46	308	5.2			

Table 2. (Continued).

Core	Section	Depth in Hole to Top of Section (m)	Interval Sampled within Section (cm)	Samples from Continuous Segment of Core	NRM Incl	NRM Decl	NRM Int	200 oe Incl	200 oe Decl	200 oe Int	$\delta = \cos^{-1} (R/N)$	Remarks	200 oe $\lvert \bar{I} \rvert$
	3	554.0	33–35		6	87	36.1	32	87	6.6			
64	1	598.5	43–45		65	88	18.4	65	86	5.0			52 ± 11
	2	600.0	115–117		37	10	20.4	44	12	5.7			
	2		121–123		78	33	9.2	61	15	3.2			
	3	601.5	118–120		42	44	17.3	45	50	4.0			
	4	603.0	126–128		41	28	18.9	43	29	5.3			
65	1	608.0	116–118		42	99	14.3	49	126	4.2			55 ± 11
	2	609.5	39–41		72	48	11.7	72	142	3.2	4°		
	2		47–49		79	102	13.2	66	160	4.4			
	2		119–121		39	294	12.7	51	284	4.1	8°		
	2		124–126		53	252	9.4	53	258	4.1			
	3	611.0	2–4		29	29	17.0	39	38	4.2	10°		
	3		6–8		64	79	12.2	56	56	4.3			
69	1	646.0	127–129		41	121	15.3	42	126	5.2	16°		34 ± 18
	1		132–134		−10	96	9.7	10	122	3.9		Continued going more normal	
	2	647.5	13–15		72	313	8.6	53	267	3.8	16°		
	2		24–26		28	221	13.6	31	233	4.9			
70	1	655.5	18–20		53	248	15.5	56	250	5.6			53 ± 3
	3	658.5	62–64		39	272	10.5	53	241	3.6	6°		
	3		78–80		67	207	13.3	51	221	4.3			
72	1	674.5	54–56		58	326	10.1	64	257	2.6			59 ± 9
	1		62–64		44	319	9.7	64	297	3.2			
	3	677.5	103–105		34	319	12.1	51	299	3.1			
	3		111–113		50	340	11.0	69	307	3.3			
	4	679.0	46–48		73	104	6.8	60	155	2.5			
	5	680.5	111–113		39	109	12.4	44	122	3.8			
	5		119–121		37	63	9.6	62	103	2.8			
73	2	685.5	120–122		69	267	12.0	58	246	3.1			53 ± 9
	2		126–128		48	306	11.6	56	259	3.4			
	3	687.0	9–11		34	6	11.9	47	11	3.0			
	3		17–19					53	10	4.3			
	4	688.5	39–41		51	345	9.1	39	357	3.2			
	4		50–52		70	14	15.0	63	7	5.0			
74	1	693.5	9–11		30	36	21.9	43	39	6.1			48 ± 6
	1		42–44		48	126	16.0	46	112	5.0			
	2	695.0	87–89		50	308	21.0	57	268	6.0			
	4	698.0	61–63		44	32	20.1	47	51	6.3			
	4		67–69		44	72	11.9	42	67	5.0			
	5	699.5	72–74		42	323	13.3	47	288	4.4			
	5		78–80		57	294	16.3	59	299	4.8			
75	2	704.5	59–61		81	342	12.3	57	320	3.5			51 ± 5
	3	706.0	10–12		63	46	12.2	52	31	4.1			
	3		18–20		38	35	9.5	47	28	3.9			
	4	707.5	94–96		61	131	10.2	57	123	3.7			
	5	709.0	78–80		43	102	12.6	44	98	4.8			
	5		87–89		51	100	11.9	51	99	4.5			
76	1	712.5	33–35		49	140	14.3	41	110	4.7			39 ± 24
	1		58–60		−78	110	15.7	−60	88	3.9			
	2	714.0	49–51		−17	178	23.1	−8	180	7.1		Going normal	
	2		53–55		61	187	8.8	46	182	4.0			
	3	715.5	103–105		65	52	14.6	41	0	7.8			
	3		110–112		79	317	25.8	76	285	6.3			
	4	717.0	4–6		−15	233	15.9	−1	246	5.7			
	4		10–12		66	293	22.3	59	278	7.4			
	5	718.5	90–92		36	218	15.8	41	225	4.7			
	5		96–98		−4	231	14.3	17	233	4.9			
77	2	723.5	50–52		45	141	13.1	51	143	3.5	20°		38 ± 9
	2		64–66		13	109	12.7	29	98	2.8			
	5	728.0	88–90		29	175	19.2	34	176	5.0	2°		
	5		97–99		29	183	18.8	36	181	5.7			
78	2	733.0	68–70		−34	209	13.4	−1	226	2.8		Going normal	26 ± 22
	2		75–77		19	8	6.6	37	24	1.2			
	4	736.0	62–64		28	109	21.9	40	73	4.1			
Mean Value													51° ± 12

Note: Lat: 23°27′, Long: 112°30′. GAD $I = 41.0°$. Present $I = 49°$. Inclination is positive downward; declination advances eastward from north, relative to the split face of the working core-half. Incl. = 0°, Decl. = 0° is horizontal and directed into the split face. The angular dispersion δ is $\cos^{-1} (R/N)$, where R is the unit-vector sum of directions for the cluster, and N is the number of samples in the cluster. The average of absolute inclinations $\lvert \bar{I} \rvert$ is also given. All angles are in degrees; intensities are in units of 10^{-7} Gauss.

The average absolute value of inclination is 51° ± 12° standard deviation, 2° standard error. The geocentric axial dipole value is 41°, and the present-day value is 49°. Interestingly, the present-day field is the one that is statistically indistinguishable from the data; in Site 467, it was the axial dipole field. Nonetheless, both of them lie within the 67% confidence interval of both data sets.

As at Site 467, a polarity stratigraphy is virtually nonexistent at Site 471. The most dramatic occurrences are a reversal pair in Core 34, Section 1 (146°angular change), and a pair of reversely polarized specimens in Core 46, Section 2.

A total of 22 specimen pairs were measured from unbroken core pieces. Similarly to Site 467, the average pair-wise dissimilarity is $\delta = 11° \pm 8°$ standard deviation. The median δ is 8.5°, equivalent to $R = 1.98°$ for $N = 2$. The crudely estimated k value is 35, corresponding to a median uncertainty of less than 12°, and a 95% uncertainty on the mean of less than 24°. The apparent uncertainties are slightly smaller at Site 471 than at Site 467. The issue of precision is again only an academic one, however, because of the obvious eradication of the original polarity recording in the sediment at both sites.

CONCLUSION

The lithified Neogene sediments at Sites 467 and 471 do not contain useful magnetic polarity stratigraphies. They are almost entirely normally polarized within middle and upper Miocene strata, rather than bearing the numerous polarity intervals characteristic of geomagnetism during that period. The average observed inclinations at the two sites are statistically identical, being 51° − 52° ± 11° − 12° standard deviation. The Site 467 value coincides with the inclination of the geocentric axial dipole field; the Site 471 value is statistically the same as the local field inclination presently. A slump fold test on Core 99 at Site 467 showed that the observed remanence was created after the folding occurred.

ACKNOWLEDGMENTS

We thank Kathy O'Neil, Ken Pisciotto, Victor Sotelo, Burt Davis, Bob Yeats, and Jack Winkle for their assistance and cooperation. We also thank Donna Allison for typing the manuscript.

This project was financially supported by the National Science Foundation, Grants OCE76-82255 and OCE78-19258. The cryogenic magnetometer was purchased through funds provided by the Woods Hole Oceanographic Institution's Ocean Industry Program.

REFERENCES

Cox, A., 1979. Confidence limits for the precision parameter. *Geophys. J. R. Astron. Soc.*, 18:545–549.

Fisher, F. A., 1953. Dispersion on a sphere. *Proc. Roy. Soc., Ser. A*, 217:295–305.

Graham, J. W., 1949. The stability and significance of magnetism in sedimentary rocks. *J. Geophys. Res.*, 54:131–167.

McFadden, P. L., 1980. Testing a paleomagnetic study for the averaging of secular variation. *Geophys. J. R. Astron. Soc.*, 61:183–192.

Ness, G., Levi, S., and Couch, D., 1980. Marine magnetic anomaly timescales for the Cenozoic and Late Cretaceous: a precis, critique and synthesis. *Rev. Geophys. Space Phys.*, 18:753–770.

Niitsuma, N., 1977. Remanent magnetization of slumped marine sedimentary rocks. *Rock Magnetism and Paleogeophysics*, 4:44–52.

Watson, G. S., 1956. A test for randomness of directions. *Monthly Notices R. Astron. Soc. Geophys. Suppl.*, 7:160–161.